



Carbon Materials from High Ash Bio-char: A Nanostructure Similar to Activated Graphene

Gu, Zhengrong^{a*}; Wang, Xiaomin^a

^a Agricultural and Biosystems Engineering Department, South Dakota State University
SAE 221, Box 2120, 1400 North Campus Drive, Brookings SD 57007, USA

ARTICLE INFO

Article history:

Received August 25, 2012

Received in revised form October 08, 2012

Accepted 12 October 2012

Available online

20 November 2012

Keywords:

Activation;
Biochar;
Activated carbon;
Grapheme;
Mesopore;
Hierarchical.

ABSTRACT

Problem statement: Developing high-value nanostructured carbon from bio-char, for electrical and natural gas energy storage, is critical to improving the economic viability of thermochemical bioenergy and biofuel conversion processes. **Approach:** We show chemical activation, using potassium or sodium hydroxide as catalysts, converted the biochar of distiller's dried grains with soluble into activated carbon with high surface area ($> 1500 \text{ m}^2/\text{g}$). **Results:** The development of porosity by chemical activation using alkali hydroxides depends on type and dosage of activation catalysts; activation temperature and atmosphere conditions. Activated carbon samples with high mesoporous volume ($>1 \text{ ml/g}$), and nanostructure similar to activated graphene were prepared at activation temperature ($1050 \text{ }^\circ\text{C}$) and KOH loading (0.05 or 0.075 mol/g biochar). **Conclusion:** This protocol offers the potential to use other protein rich feedstocks for preparing nanostructured carbon, containing nanostructure similar to activated graphene, as an advanced carbon material.

© 2013 Am. Trans. Eng. Appl. Sci.



1. Introduction

Renewable lignocellulosic biomass, such as native grasses, as well as agricultural crop residues including corn stover, can be converted to drop-in biofuels through thermochemical processes. Because of the lower reaction time and fewer pretreatment requirements, thermochemical processes are more efficient than bio-chemical/biological processes. All thermochemical bioenergy conversion processes, including gasification, hydrothermal pyrolysis, fast pyrolysis and slow pyrolysis, generate a solid co-product called bio-char. The bio-char generated from fast pyrolysis has a significantly higher ash content than charcoal obtained through traditional carbonization processes. So far, bio-char generated in thermochemical conversion has only been used as a soil amendment or low grade fuel (Brewer et al. 2008; Wang et al. 2009), which inherently limits the market demand for this type of char. Therefore, developing high-value *co-products* from bio-char is necessary to improve the economic sustainability and viability of thermochemical bioenergy and biofuel conversion processes.

Activated carbon is one possible high-value co-product (\$1100 US/ton in 2007) with demands growing 9% annually through 2017 (Marsh and Rodriguez-Reinoso 2006; GIA 2012). In the activated carbon industry, physical activation by using gasifying agents, carbon dioxide and water vapor (either singly or together) and chemical activation by using potassium/sodium hydroxides or their carbonates are well established for activation of pyrolyzed biomass (charcoal or bio-char) from woody biomass such as coconut shell or hardwood. In research, bio-char from fast pyrolysis of wood, or corn cob containing less than 20% ash, has been successfully converted to activated carbon with surface area $>1000 \text{ m}^2/\text{g}$ through physical activation with CO_2 (Zhang et al. 2004), and chemical/catalytic activation with KOH (Azargohar and Dalai 2008), while most fast pyrolysis bio-char, from herbaceous biomass, were only successfully upgraded to activated carbon with low surface area (around $600 \text{ m}^2/\text{g}$) with physical activation (Zhang et al. 2004; Lima et al. 2010). However, dehydrating agents, such as ZnCl_2 and H_3PO_4 , are not suitable for activation of carbonized feedstock (Marsh and Rodriguez-Reinoso 2008; Gu et al. 2008) such as bio-char (results not reported here).

Currently, high surface ($>2000 \text{ m}^2/\text{g}$) activated carbon, from sustainable resources, is attracting more attention because of a fast growing market for electrical energy and natural gas

storage. Likewise, activated carbon with high surface area ($>2000 \text{ m}^2/\text{g}$) has been prepared successfully from herbaceous biomass such as peanut shell (Ioannidou and Zabaniotou 2007), rice husk /straw (Zhang et al. 2009), sewage sludge (Lillo-Rodenas et al. 2008), corn cob (Aworn et al. 2009), using NaOH, KOH or carbonates of alkali metals as activation agents. However, bio-char, after recovering biofuel or bioenergy, is different from biomass. The much higher mineral (ash) content in these bio-chars creates a significantly different challenge for preparing high quality activated carbon. In most herbaceous bio-char, major ash components are silica or silicate derivatives followed by oxides of alkalis (Brewer et al. 2008). Soluble ash components (e.g., carbonates and oxides of alkali metals, alkali earth metals and oxides of transition metals) in herbaceous bio-chars are particularly effective positive catalysts for gasification of carbon using steam or carbon dioxide (Marsh and Rodriguez-Reinoso 2008; Gu et al. 2008). For example, only trace (about 1% wt) alkali and alkali earth metal oxidants in bio-chars catalyze combustion reaction with steam or oxygen 10 times faster (Matsumoto et al. 2010), while insoluble silica ash components in biomass or high ash bio-char has been used as a natural template for controlling the pore structure of activated carbon in chemical activation catalyzed by hydroxide or carbonates of alkali metal (Yeletsky et al. 2009).

Corn ethanol is the major biofuel in USA, which generate distiller's dried grains with solubles (DDGS) as major co-product. DDGS, containing mainly protein, fiber and fat, is generally used as an additive for animal feeds. DDGS was also used as potential energy sources for producing bio-oil with about 67% heating value of gasoline through thermochemical processes (Lei *et al.* 2011), which also generated 20~30% bio-char containing around 50% ash and minerals. Bio-char of DDGS is far different from the char of other biomass such as crops residues and energy crops. Although high surface area activated carbon has been prepared from bread yeast residues using alkali metal carbonates as activation agents (Urabe et al. 2008), bio-char of DDGS, after biooil recovery, has not been utilized in carbon materials preparation.

In this study, bio-char from DDGS after pyrolysis, which was a co-product produced by thermochemical processing designed for maximum bioenergy production, was collected and chemically activated using KOH and NaOH as catalysts. Activated carbon samples were

characterized using different analytic approaches (e.g., Scanning Electron Microscopy (SEM), Raman Spectroscopy, N₂ isothermal adsorption, and XRD and TEM). This study aimed to evaluate impact of activation parameters, (i.e., catalysts type, ratio of base to char, atmosphere during activation, and temperature) on properties of generated activated carbon.

2. Materials and Experimental Methodology

2.1 Materials

Bio-char of DDGS was used as feeding material for activation. This bio-char was produced from biomass using pyrolysis process. See the compositions and properties of the bio-char listed in Table 1. Table 2 gives Mineral ash composition in bio-char of DDGS.

Table 1: Compositions and properties of bio-char sample.

Biomass	Volatile % dry	Moisture %	N% dry	C% dry	C/N	Ash%dry (575 C for 24 hr)	Density (apparent)	surface area m ² /g
DDGS	9.3	4.4	8.27	60.73	7.27	47.42	0.36	7.77

Table 2: Mineral ash composition in bio-char of DDGS.

Mineral	Ca	P	K	Na	Mg	Fe	S
% in ash	28	8	2	2	2	15	1.5

2.2 Activation

NaOH and KOH were used as catalysts for chemical activation in N₂ inert atmosphere. Bio-char samples were mixed with solution of catalysts and dried in a conventional oven at 120 °C overnight. These dried mixtures were further dried at 400 °C in a muffle furnace (chamber is 15*15*22 cm) in N₂ atmosphere (N₂ flow is 500 ml/min) for more than 2 hours to remove crystal water. Then, activation was carried out at specific temperatures for a certain amount of time. After specified activation time, activated samples were cooled within muffle furnace in same N₂ atmosphere. The control experiments without N₂ flow were also tested with a KOH catalyst.

After activation, activated carbon samples were washed with 0.1 mol/L HCl at 100 °C with condensing, then washed with DI water to pH 7 and dried at 105 C overnight under vacuum.

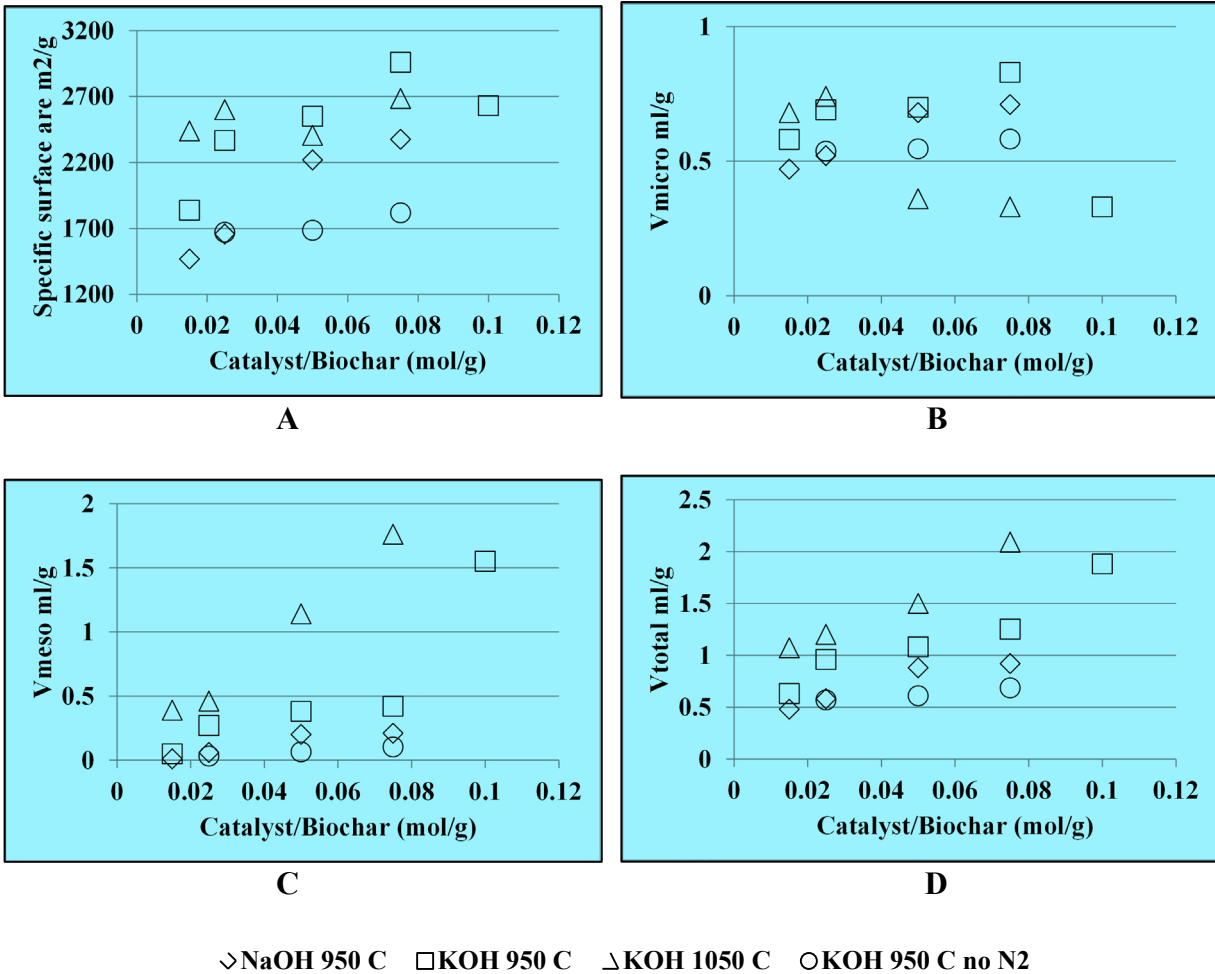


Figure 1: Catalysts load and activation.
A: Surface Area, **B:** Micropore Volume, **C:** Mesopore Volume, **D:** Total Pore Volume

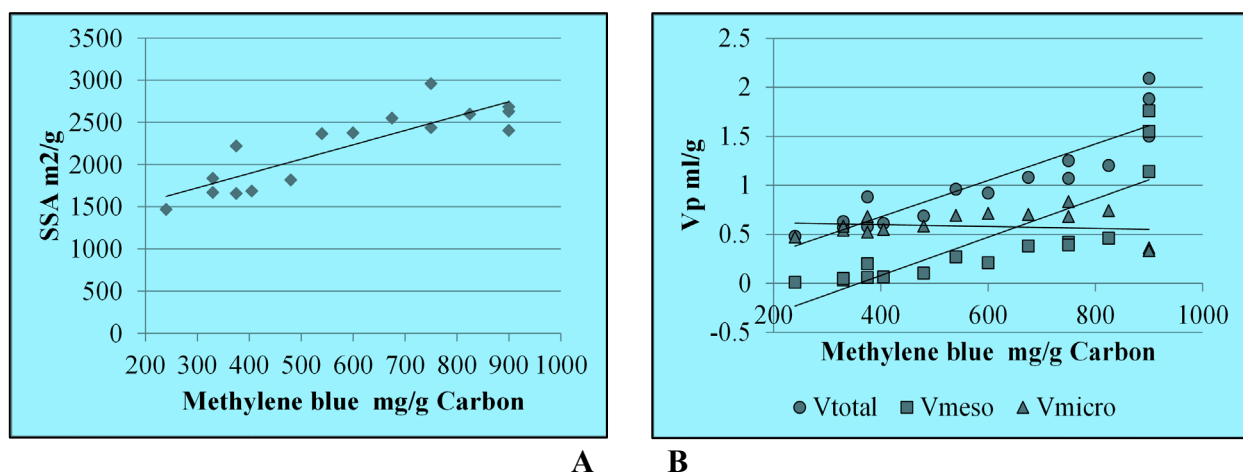
2.3 Analytical methods for bio-char and activated carbon samples

Isotherm adsorption of N₂ at 77K was carried out using Surface Area and Pore Size analyzers (one ASAP 2010 Micropore analyzer). The specific surface areas were calculated using the Brunauer–Emmett–Teller (BET) equation. The total pore volumes were obtained at relative pressure 0.99 P₀. The micropore volume was estimated using *t*-plot method, while mesopore volume and the pore size distribution were determined by the NLDFIT analysis for carbon with slit pore model (Micromeritics Inc.) based on the N₂ isotherm adsorption data.

The methylene blue adsorption was analyzed according to standard protocol described in

reference (Marsh and Rodriguez-Reinoso 2008; Gu et al. 2008). For brief, specific volume methylene blue solution 1.5 g/L in phosphate buffer (3.6 g KH_2PO_4 and 14.3 g Na_2HPO_4 in 1 L water, pH=7, no titration is permitted) was added to 0.1 g dried activated carbon (>90% pass 200 mesh or 71um screen) and incubated for 10 minutes on shaker (275 rpm) at 25 C. The slurry was centrifuged at 5000 rpm for 5 minutes and filtrate with filter paper. The clarified sample was quantified with spectrophotometer at 665 nm (1cm cuvette). If the Ab of light was the same as CuSO_4 solution (2.4g $\text{CuSO}_4 \cdot 5\text{H}_2\text{O}$ in 100 ml water), the specific volume of methylene blue was used to calculated adsorption amount. If the Ab of light was higher than CuSO_4 solution, the methylene blue solution volume was reduced and the assay was redone.

Mineral composition in carbon samples were identified and quantified with inductively coupled plasma–atomic emission spectrometry (ICP-AES Varian 735-ES). The structure of activated carbon was also characterized with Raman Spectrum (Horiba LABRam confocal Raman microscope) at room temperature, using an excitation wavelength at 532 nm from a diode pumped solid-state laser, as well as TEM (Hitachi H-7000 FA) and XRD (Rigaku D/Max Ultima).



Supplement Figure 1:

A: Methylene blue Adsorption and Surface Area, **B:** Methylene blue Adsorption and Pore Volume.

3. Results and Discussion

3.1 Bio-char properties

The ash content of DDGS bio-char used in this project is higher than 45%wt, while its BET surface area is less than 10 m²/g. After activation, the apparent bulk density of activated carbon is around 0.2 g/cm³ as same as activated carbon from coal using KOH at the same molar ratio to char.

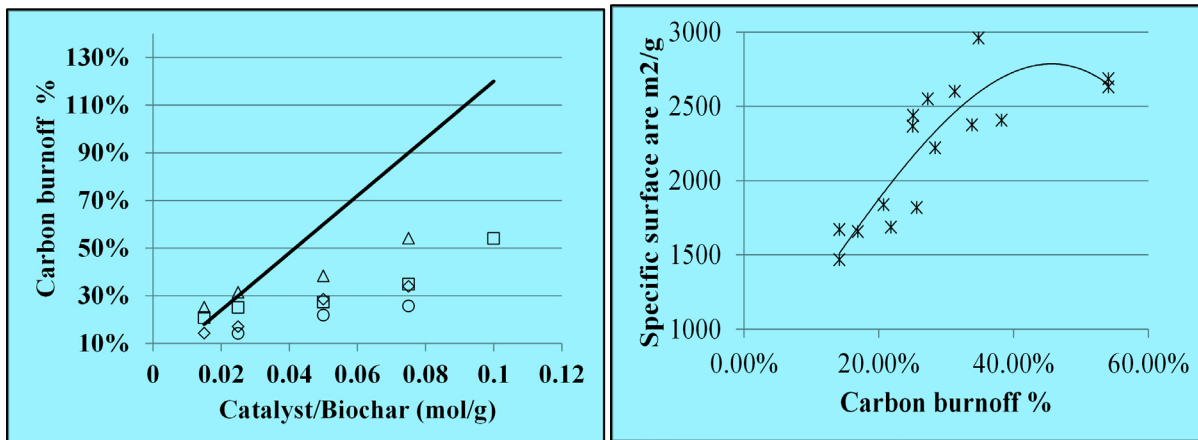
3.2 Impact of activation parameters

For both activation catalysts, the dosage of the activating agent changed the surface area of the activated carbons derived from DDGS bio-char. For activation with KOH at 950 °C, the BET surface area increased with the increase in the dosage of KOH, until the molar/mass ratio of base/bio-char reached 0.075, and then decreased slightly; while BET surface area just fluctuated around 2500 m²/g for activation using KOH at 1050 °C. For activation with NaOH at 950 °C, BET surface area increased with the increase in the dosage of the catalyst (Figure 1A). Microporous volume also heavily depends on temperature and catalysts loading, (i.e., increased with dosage of KOH and NaOH), until the molar/mass ratio of base/bio-char reached 0.075 at 950 °C. But at 1050 °C, microporous volume decreased heavily at high KOH loading (> 0.05 mol/g) (Figure 1B). However, the total pore volume and mesopore volume increased with dosage of catalysts (Figure 1C&D).

Those results could be explained according to mechanism of base activation (Alcañiz-Monge and Illán-Gómez 2008; Lillo-Rodenas et al. 2003); the carbon burnoff increased with catalyst loading and temperature (Figure 2A) because reactions between carbon and sodium or potassium hydroxide are more favored at higher temperatures and high activation agent loading. Therefore, the BET surface area increased with carbon burnoff until around 40% (Figure 2B). However, further increasing KOH loading caused more severe burnoff of the surface carbon atoms through carbon gasification reactions with activation agent KOH and activation products, such as K₂CO₃, K₂O, CO₂ and H₂O, as well as lead to a decrease of the surface area of the porous carbon and damaged the structures of micropores. As the result, micropore volume increased slightly to <40% carbon loss (Figure 2C) then decreased with further carbon burnoff, while meso and total pore volume increased with carbon burnoff. Additionally, the carbon loss or burnoff increased sharply

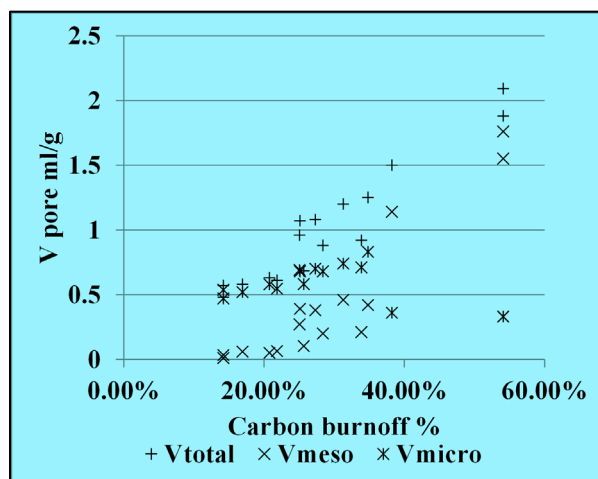
when the ratio of KOH/bio-char increased from 0.075 to 1 mol/g because gasification of carbon with KOH is a self-catalytic reaction catalyzed by KOH. Furthermore, the reaction rates of all of those reactions were faster at higher temperatures. As a result, the activation at a temperature of 1050 °C generated higher specific surface area at lower KOH loading (i.e., 0.015 and 0.025 mol KOH/g bio-char), while causing a lower specific surface area at higher KOH loading (i.e., 0.05 and 0.075 mol KOH/g bio-char) (Figure 1A). Activated carbon with less micropores as well as higher percentage of mesopore was obtained at higher KOH dosage and temperature (Figure 1C&D), which are attributed to predominating of pore widening at higher base loading (Alcañiz-Monge and Illán-Gómez 2008; Lillo-Rodenas et al. 2003) and gasification on the external surface of the carbon which destroy the porous structure. This result was also verified by pore size distribution obtained through NLDFT analysis for isothermal N₂ adsorption data with slit pore model (Fig 3A, B and C). Pore size increased with KOH/NaOH dosage and temperature. It was noteworthy that activated carbon samples, catalyzed using NaOH, showed lower specific surface area and porous volume than samples prepared with KOH at the same temperature and molar dosage (Figure 1). This is similar to results obtained in activation of low rank coal (Alcañiz-Monge and Illán-Gómez 2008; Lillo-Rodenas et al. 2003) and lignin (Fierro et al. 2007) with NaOH and KOH, because KOH is a stronger oxidant and dehydrator than NaOH, (i.e., KOH begins reacting with not completely carbonized carbon at 400 °C, which is lower than NaOH at ~570 °C). The Bio-char of the DDGS used in this project is similar to low grade coal containing high amounts of nitrogen, as well as significant hydrogen and oxygen.

Furthermore, activated carbons prepared at 1050 °C with KOH loading at 0.05 or 0.075mol/g or synthesized at 950 °C with higher KOH (i.e., 0.1 mol/g) loading showed nitrogen isothermal adsorption similar to activated graphene (Zhu et al. 2011), which also showed the hysteresis loop between adsorption and desorption isotherms (Figure 4A&B), as the evidence for the existence of slit mesopores (Figure 3 A&B) between graphene nanosheets (Zhu et al. 2011). In this research, mesopore structure was also shown through methylene blue adsorption analysis (Supplement Figure 1). However, methylene blue adsorption depends more on surface area and total pore volume due to its molecular size (1.43 nm × 0.61 nm × 0.4 nm). Therefore, in contrast to ASTM methods, methylene blue adsorption is a useful method for estimating activation efficiency, surface area, and total pore volume, but is not an accurate tool to quantify or estimate mesoporous pore volume.



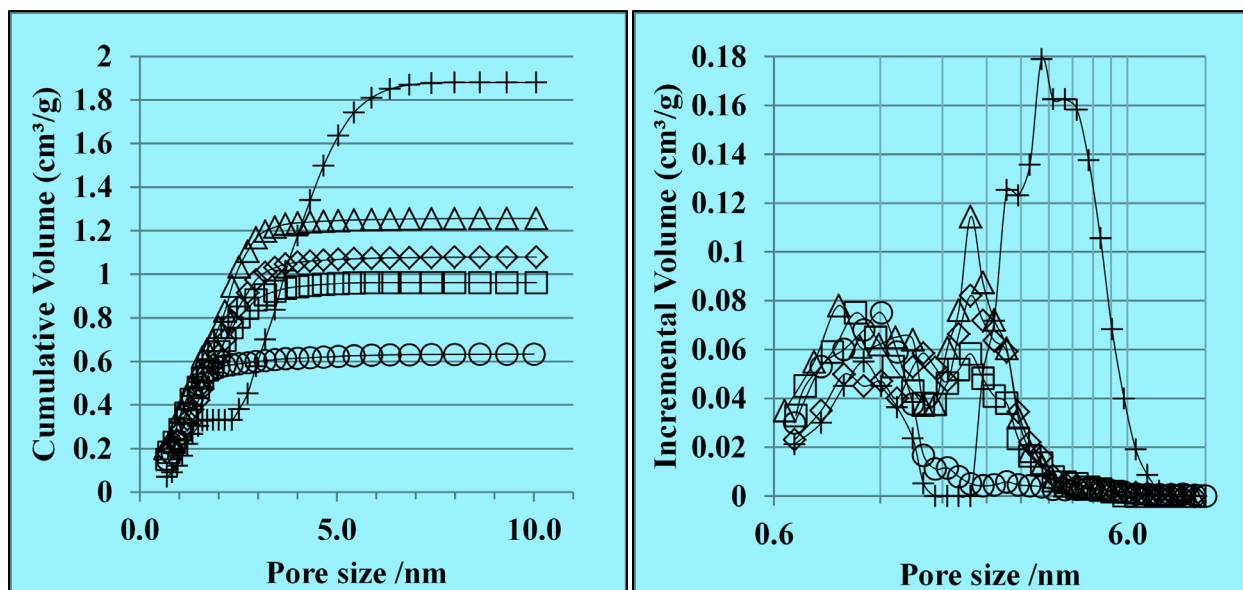
A B

◇ NaOH □ KOH 950 C △ KOH 1050 C ○ KOH 950 C no N₂ — Estimated

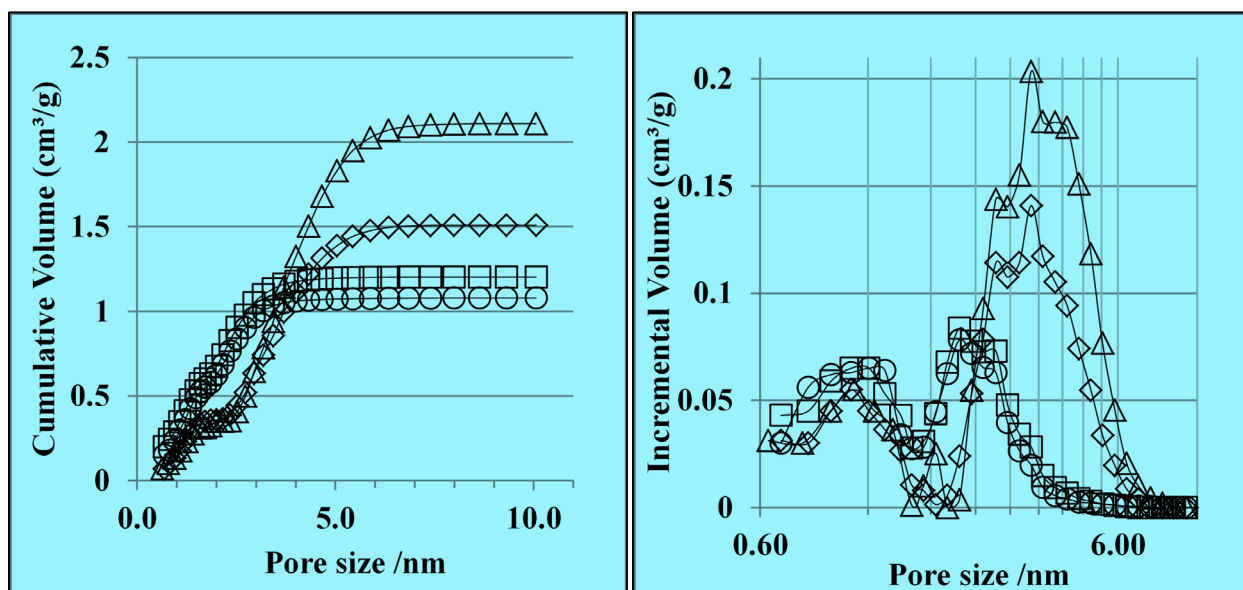


C

Figure 2: Carbon burnoff and activation
A: Catalysts load and Carbon Burnoff
B: Surface Area and Carbon Burnoff
C: Pore Volume Carbon Burnoff.



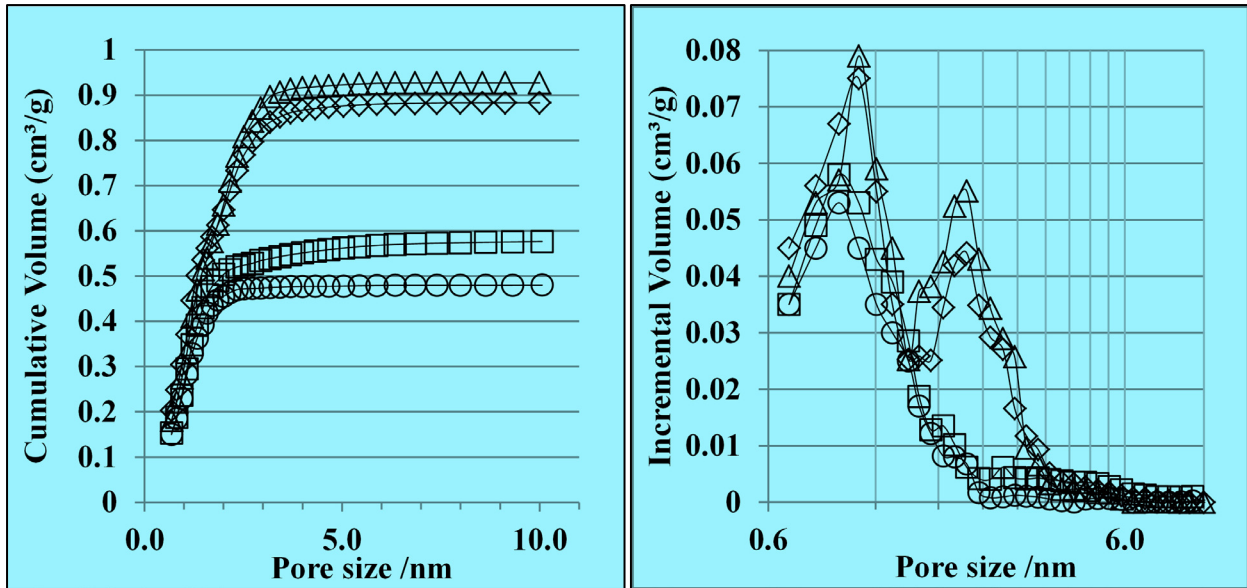
A



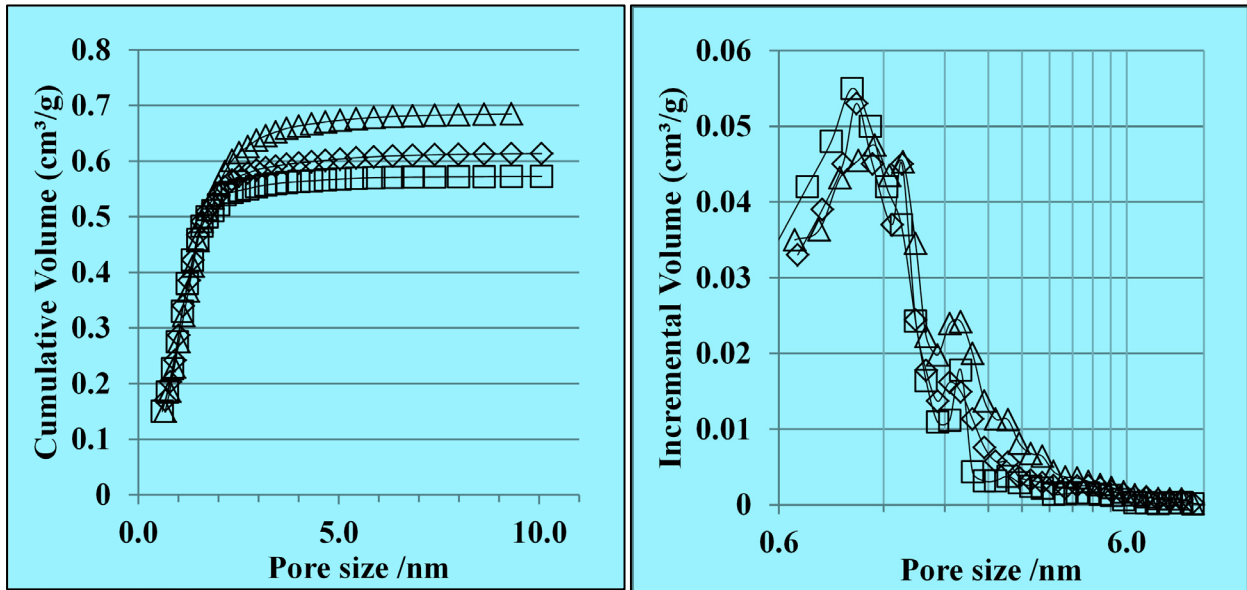
B

○ 0.015 □ 0.025 ◇ 0.05 △ 0.075 + 0.1

Figure 3. Pore Distribution for Activated Carbon from DDGS Biochar
A: KOH 950 °C, B: KOH 1050 °C



C



D

—○— 0.015 —□— 0.025 —◇— 0.05 —△— 0.075 —+— 0.1

Figure 3 (continued): Pore Distribution for Activated Carbon from DDGS Biochar
C: NaOH 950 °C, **D:** KOH 950 °C without N₂ flow.

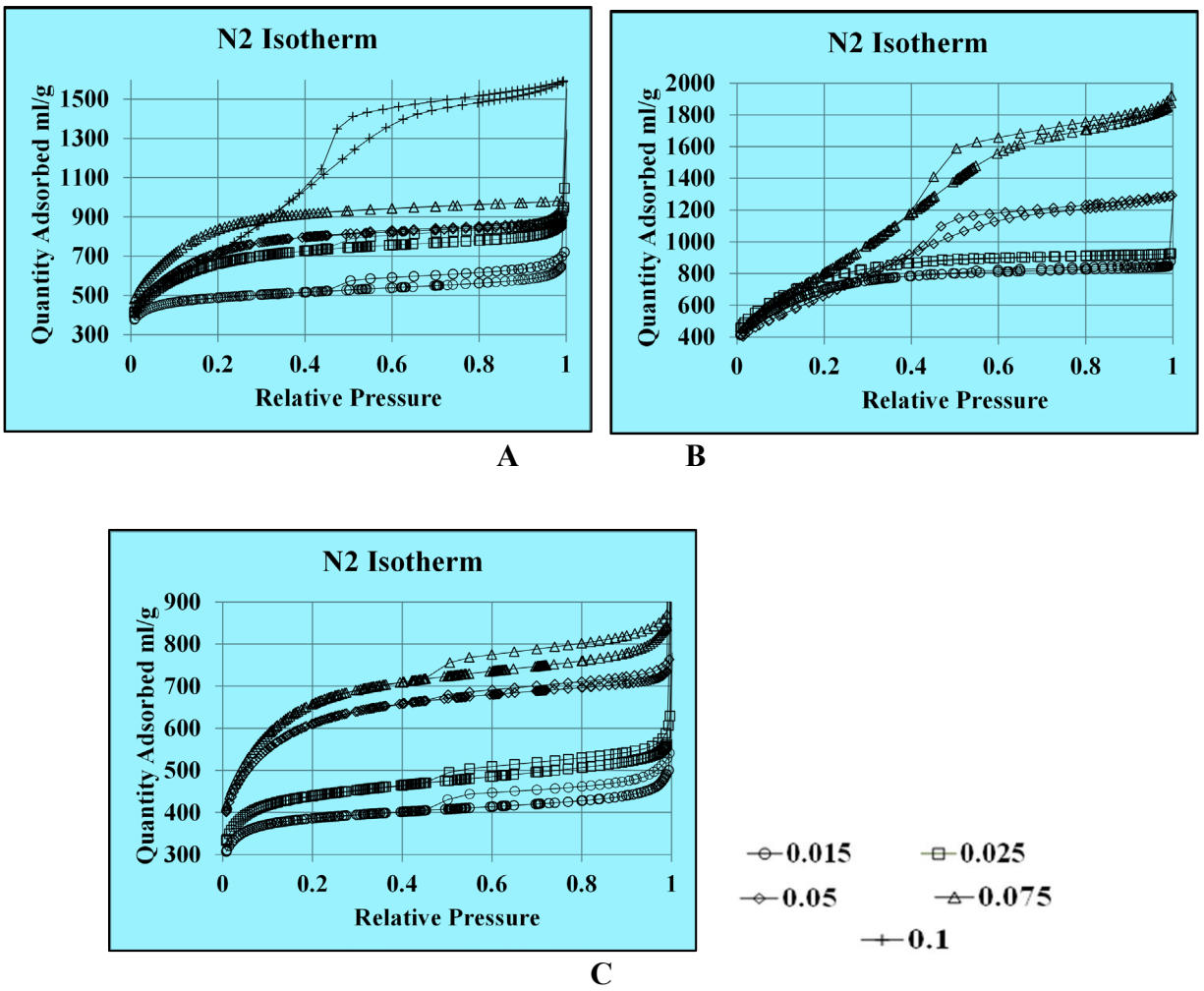


Figure 4. N₂ isothermal for Activated Carbon from DDGS Biochar
 A: KOH 950, B: KOH 1050, C: NaOH 950.

Experimental results also showed the significant impact of nitrogen flow on activation at 950 °C using KOH as a catalyst; without nitrogen flow, the surface area and pore volume are significantly lower, even lower than activation using NaOH as catalyst with nitrogen flow (Figure 1A). However, the carbon yield was higher without nitrogen flow (Figure 2A). According to published reports of the activation mechanism in KOH or NaOH activation, nitrogen flow can remove gas products generated during activation, including inhibitive products such as H₂ and CO, as well as reduce potential activation agents such as vapor of hydroxides, steam and CO₂ (Alcañiz-Monge and Illán-Gómez 2008; Lillo-Rodenas et al. 2003; Fierro et al. 2007). Therefore, without nitrogen flow, the atmosphere in closed chamber became H₂ and CO rich, which inhibited further activation reactions between carbon and hydroxide catalysts.

3.3 Activation mechanism of high ash bio-char

On the other hand, in chemical activation with KOH or NaOH, the activation mechanisms to generate porous structure are complicated. If all porous structure was caused by carbon gasification, according to the stoichiometry of gasification reactions listed below, the carbon burnoff should increase linearly with catalysts loading. However, the burnoff of carbon was significantly lower than calculated value at higher catalysts dosage, which is estimated according to mechanism listed in below (Figure 2A). Therefore, the activation mechanism with NaOH/KOH is not only due to gasification of carbon through reaction with catalysts and derivative product (reactions 1-6), but also due to intercalation, which must play an important role on nano-porous structure formation. A similar result was also verified by Alcañiz-Monge and Illán-Gómez (2008), where carbon, activated with NaOH, showed a much higher surface area and pore volume than carbon activated with steam or CO₂ at comparable carbon burnoff because of the intercalation/de-intercalation of metallic generated during activation.



Where Me is alkaline metal element, such as Na and K.

Besides reactions involving carbon and intercalation, the reaction among ash components with catalysts are significant for forming porous structure. For example, after activation, specific surface area of carbon samples, activated with NaOH at 0.025mol/g, was only around 300m²/g before ash removal, while surface area of activated carbon samples increased to more than 1500 m²/g after further ash removal, i.e. water washing followed by HCl washing to remove soluble compounds. Furthermore, specific surface area of control samples after heat treatment and ash

removal without activation agent was only $30\text{m}^2/\text{g}$.

According to the results obtained in this research, the activation of bio-char with alkaline hydroxide includes multiple processes: dehydration and dehydrogenation of non-carbonized components; gasification of carbon with catalysts and derivative product; intercalation of metallic species. In addition, soluble compounds, formed through reaction among ash components with catalysts, are templates for forming porous structure after dissolving in washing steps. As a result, the development of porosity in bio-char by chemical activation using alkali hydroxides depends on several interrelated parameters: ash compositions and distribution in bio-char; initial porous structure of bio-char; type and dosage of activation catalysts; activation temperature; time; atmosphere conditions.

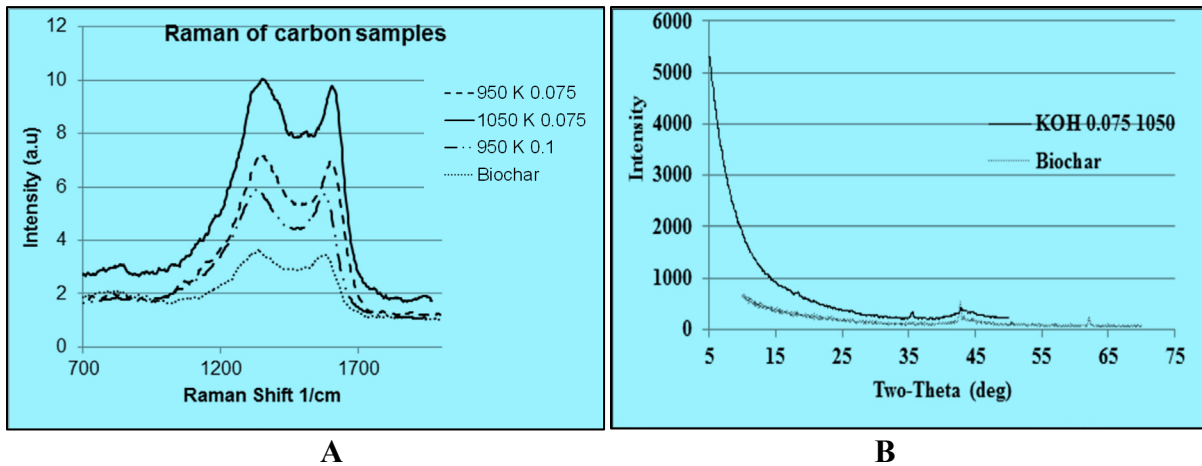


Figure 5. A: Raman of Activated carbon, B: XRD of Activated carbon

3.4 Activated graphene similar structure in nanostructured activated carbon

It is also noteworthy that DDGS bio-char based nanostructured activated carbon is different from traditional activated carbon. The most important difference is that nanostructured activated carbons, prepared at $1050\text{ }^{\circ}\text{C}$ with KOH dosage at 0.05 or 0.075 mol/g or at $950\text{ }^{\circ}\text{C}$ with KOH loading 0.1 mol/g, showed significant slit mesopores structure (Figure 3 A&B). The Raman spectrum of the activated carbons, based on DDGS bio-char, also exhibited two peaks at $1580/\text{cm}$ (G band) and $1360/\text{cm}$ (D band). Both G and D bands are generally caused by sp^2 -bonded carbon. The D-band is usually related to the existence of disordered turbostratic/defective and non-graphitic carbon, while the G-band, as the graphitic band, corresponds to an intermolecular

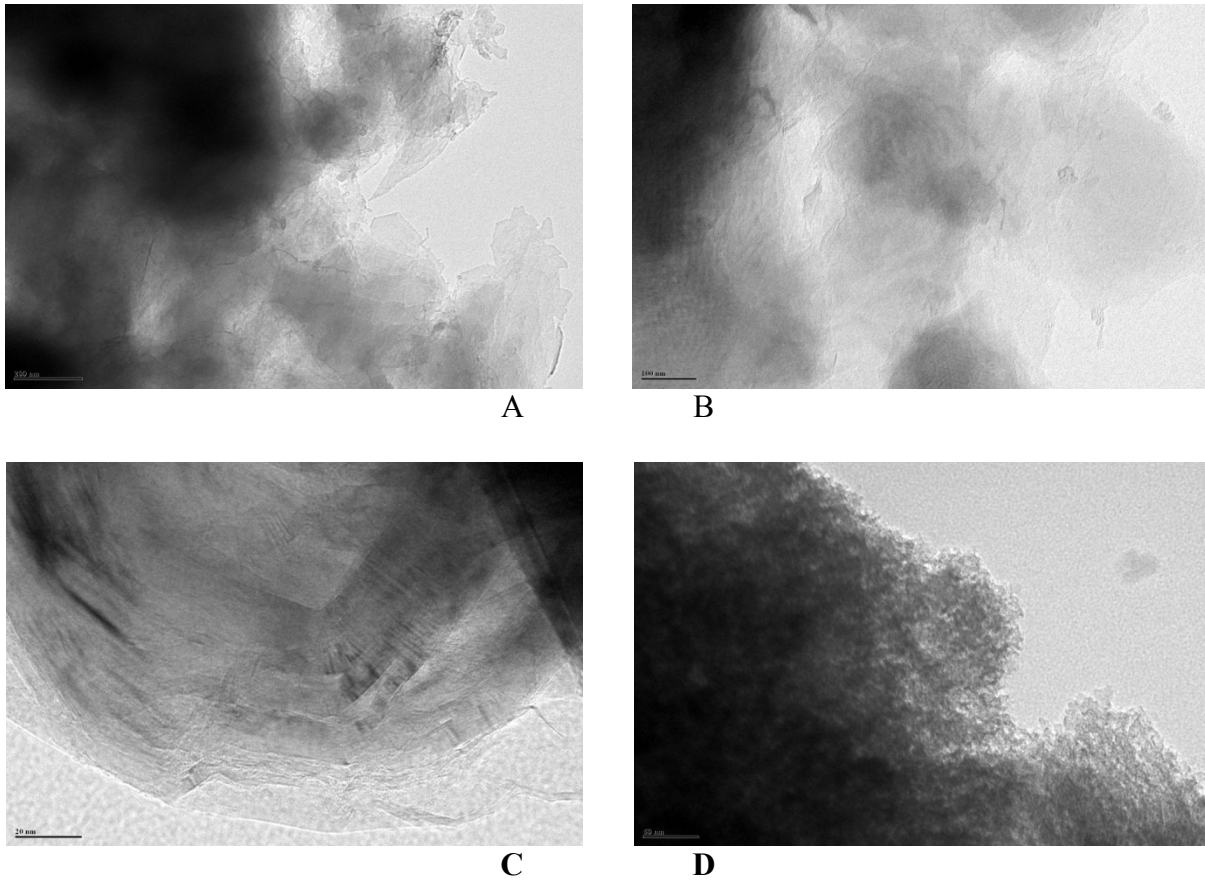


Figure 6: TEM of Activated carbon from DDGS biochar (KOH 0.075 1050 °C).
A: TEM at 300 nm, **B:** TEM at 100 nm,
C: TEM at 20 nm, **D:** TEM of commercial activated carbon at 50 nm

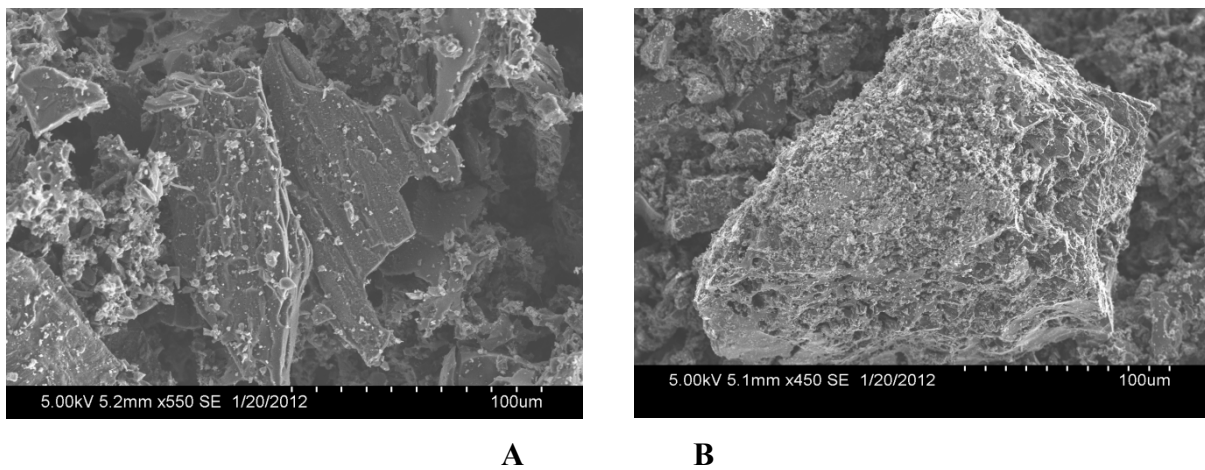


Figure7. SEM image of biochar and activated carbon from DDGS
A: Biochar of DDGS **B:** Activated carbon (KOH 0.075, 1050 °C)

shear vibration of carbon atoms between individual C-layers (Oskar *et al.* 2005). In the present work, the Raman spectrum result showed characters corresponding to individual graphene nanosheet structure, and the disordered and imperfect structures of carbon materials in the activated carbon respectively. In addition, it is noteworthy that the I_d/I_g of activated carbon, activated with KOH at 1050 °C is 1.06 (Figure 5A), is similar to the value reported for activated graphene (Zhu *et al.* 2011). The XRD result of the activated sample (Figure 5B) also showed similarity to activated graphene (Zhu *et al.* 2011); there are no peaks related to carbon crystal structures. This result is consistent with the observations from TEM. The high-resolution TEM image clearly shows the micro-graphene structure within the activated carbon materials based on DDGS bio-char. Furthermore, different from traditional activated carbon (Figure 6D), distinct domains of graphene sheets or layers structure are observed in the TEM images (Figure 6 A&B). The metrical thickness value is around 0.4 nm, which is close to the theoretical value (0.34 nm) of single-layer graphene (Figure 6C). As a result, single graphite or graphene layer is obtained from DDGS bio-char after activation with KOH. This observation was not expected, even X-ray scattering already showed the existence of turbostratic disordered graphene stacks embedded in amorphous phases in bio-char, which is generated from pyrolysis processes of lignocellulosic biomass (Oskar *et al.* 2005; Keiluweit *et al.* 2010). Although the micropores in activated carbon are formed through random cross-linking of graphene micro-sheets in the porous carbon, individual graphene nanosheets do not exist in general activated carbon (Figure 6D) or bio-char (Marsh and Rodriguez-Reinoso 2006; Malard *et al.* 2009). In addition, KOH activation resulted in layers carbon structure from DDGS bio-char particles (Figure 7A & B).

Therefore, the mechanism to form graphene structure in activated carbon, which is produced from bio-char of DDGS with KOH activation, needs further investigation. On the other hand, carbon materials with structure similar to graphene or oxidized graphitic sheets have been synthesized from biobased organic compound using mesopore silicate or silica as templates (Clippel *et al.* 2011). The graphene-like conductive carbonaceous structure, supported on silica or silicates was obtained from pyrolysis, at 800°C in N₂ without reducing agents, of compounds containing clay or sepiolite and carbon precursor such as sucrose, caramel or gelatin, while only aggregates of graphene sheets were produced without porous silicate supports (Eduardo *et al.* 2011;

Gmez-Avils et al. 2007). Furthermore, N-doped carbonaceous porous nano-sheets had been synthesized from collagen cross-linked gel after pyrolysis in nitrogen atmosphere (Lee et al. 2011). According to these reported results and samples obtained in our lab, protein rich precursors (i.e., DDGS and high ash content in DDGS's bio-char) are possible major factors in forming activated graphene like structure in prepared activated carbon samples.

Until now, graphene is generally produced from graphite through a similar method (i.e., breaking graphite into oxidized graphite nanosheets with strong acid and strong oxidants), which was developed by Hummers and Offeman (1958), after that oxidized graphite nanosheets are dispersed by ultrasonic stirring and reduced to graphene with hydrazine, hydrogen, or electrochemical reduction (Regis et al. 2010). Although graphite based graphene has been manufactured in pilot scale (i.e., 10 ton/year with lower cost approaches), the price is still prohibitively high (more than \$ 200/kg, XGScience Inc) for a large scale application (Segal 2009). On the other hand, bottom-up approaches to direct synthesis graphene nanosheets from organic compounds, such as solvent-thermochemical reduction of organic compounds with metal sodium (Choucair et al. 2009), are still in early stages and limited by conversion ratio and costs.

4. Conclusion

We prepared a super activated carbon that has a nanostructure similar to activated graphene and potentially offers a lower cost substitute for the advanced carbon materials currently derived from graphene or activated graphene. According to Raman, TEM and XRD and N₂ isothermal adsorption results, the nanostructure similar to activated graphene was domain portion in the overall structure, which was also verified by energy storage capacity of the carbon materials. Especially as an advanced carbon material, the super activated carbon with graphene-like nanosheets has excellent potential as high capacity anode materials for lithium batteries or supercapacitors (Gerard and Tarun 2011) and as adsorbents for natural gas or hydrogen storage. Our super-capacitor, using 6mol/L KOH as electrolyte and electrodes composed of activated carbon prepared with KOH (0.075 mol/g) activation at 1050 °C, showed stable high reversible capacity (i.e., 270 F/g at constant currents 1A/g), while the capacity is 160 F/g at constant currents

1A/g using organic electrolytes i.e., 1 mol/L TEA BF₄ in acetonitrile (results not discussed here).

5. Acknowledgement

This research is funded by project “DEVELOPMENT OF HIGH VALUE CARBON BASED ADSORBENTS FROM THERMOCHEMICALLY PRODUCED BIOCHAR” 2011-67009-20030 USDA-NIFA Agriculture and Food Research Initiative Sustainable Bioenergy Program.

6. References

- Alcañiz-Monge J., Illán-Gómez, M.J. (2008), Insight into hydroxides-activated coals: Chemical or physical activation, *J. Colloid and Interface Sci.* 318, 35–41
- Aworn A., Thiravetyan P., Nakbanpote W., (2009), Preparation of CO₂ activated carbon from corncob for monoethylene glycol adsorption, *Colloids and Surfaces A: Physicochem. Eng. Aspects* 333, 19-25
- Azargohar R., Dalai A.K.,(2008), Steam and KOH activation of biochar: Experimental and modeling studies, *Microporous and Mesoporous Materials* 110, 413-421
- Brewer C.E., Schmidt-Rohr K., Satrio J.A., Brown R.C., (2008) Characterization of Biochar from Fast Pyrolysis and Gasification Systems, *Environmental Progress & Sustainable Energy*, 28, 386-396.
- Choucair M., Thordarson P., John A. (2009), Stride Gram-scale production of graphene based on solvothermal synthesis and sonication,; *Nature Nanotechnology*, 4, 30-33.
- Clippel F, Harkiolakis A., Vosch T., Ked X., Giebeler L., Oswald S., (2011), Graphitic nanocrystals inside the pores of mesoporous silica: Synthesis, characterization and an adsorption study, *Microporous and Mesoporous Materials*, 144,120–133
- Eduardo RH, Margarita D, Francisco MF, Ezzouhra Z, (2011), Supported Graphene from Natural Resources: Easy Preparation and Applications, *Adv. Mater.*, 23 , 5250-55
- Fierro V., Torne´-Ferna´ndez V., Celzard A., (2007), Methodical study of the chemical activation of Kraft lignin with KOH and NaOH, *Microporous and Mesoporous Materials* 101, 419–431
- Gerard KS, Tarun G, (2011), Improving Anodes for Lithium Ion Batteries, *Metallurgical & Materials Transaction A*, 42, 231-238
- Gmez-Avils A., Margarita D., Aranda P., Eduardo RH, (2007), Functionalized Carbon–Silicates from Caramel–Sepiolite Nanocomposites, , *Angew. Chem. Int. Ed.* 2007, 46, 923 –925
- GIA (2012) Activated Carbon: A Global Strategic Business Report, Feb. 2012, Global Industry

Analysts; http://www.prweb.com/releases/activated_carbon/water_treatment/prweb8286149.htm

Gu K.L., Gu Z.R., Li G.J. (2008), Application of Activated Carbon, China Educational Science Publishing House. Beijing, China.

Hummers WS and Offeman RE, (1958), Preparation of graphitic oxide J. Am. Chem. Soc. 1 1339

Ioannidou O., Zabaniotou A., (2007), Agricultural residues as precursors for activated carbon production - A review, Renewable and Sustainable Energy Reviews, 11, 1966-2005

Keiluweit M; Nico PS.; Johnson MG., (2010), Dynamic Molecular Structure of Plant Biomass-Derived Black Carbon (Biochar), Environ. Sci. Technol. 44, 1247–1253

Lee YH, Lee YF, Chang KS, Hu CC, (2011), Synthesis of N-doped carbon nanosheets from collagen for electrochemical energy storage/conversion systems, Electrochemistry Communications 13, 50–53

Lei HW; Ren SJ; Wang L, (2011), Microwave pyrolysis of distillers dried grain with solubles (DDGS) for biofuel production, Bioresource Tech., 102, 6208-6213

Lillo-Rodenas M.A., Cazorla-Amoros D., Linares-Solano A., (2003), Understanding chemical reactions between carbons and NaOH and KOH, An insight into the chemical activation mechanism, Carbon, 41, 267–275

Lillo-Rodenas MA, Ros A., Fuente E, Montes-Mor'an MA, Martin MJ, Linares-Solano A, (2008), Further insights into the activation process of sewage sludge-based precursors by alkaline hydroxides, Chem. Eng. J. 142, 168–174

Lima IM, Boateng AA, Klasson KJ. (2010), Physicochemical and adsorptive properties of fast-pyrolysis bio-chars and their steam activated counterparts, J Chem Technol Biotechnol, 85, 1515–1521

Malard L.M., Pimenta M.A., Dresselhaus G., Dresselhaus M.S., (2009), Raman spectroscopy in graphene,; Physics Reports 473, 51-87

Marsh H., Rodriguez-Reinoso F.,(2006) Activated Carbon, ISBN: 0080444636; Pub. Date: August 2006, Publisher: Elsevier Science & Technology Books, London, British.

Matsumoto K., Takeno K., Ichinose T., Ogi T., Nakanishi M. (2010), Behavior of Alkali Metals As the Carbonate Compounds in the Biomass Char Obtained As a Byproduct of Gasification with Steam and Oxygen at 900-1000 °C, Energy Fuels, 24, 1980-1986

Oskar P., Zollfrank C., Zickler GA, (2005), Decomposition and carbonisation of wood biopolymers—a microstructural study of softwood pyrolysis, Carbon, 43, 53–66

Raposo F., Rubia M.A., Borja R., (2009), Methylene blue number as useful indicator to evaluate

the adsorptive capacity of granular activated carbon in batch mode: Influence of adsorbate/adsorbent mass ratio and particle size, *Journal of Hazardous Materials*, 165, 291-299

Regis YN G, Konstantinos S, Rudolf P., (2010), A roadmap to high quality chemically prepared graphene, *J. Phys. D: Appl. Phys.* 43, 4015-4033.

Segal M. (2009), Selling graphene by the ton, *Nature Nanotechnology*, 4, 612-614

Urabe Y., Ishikura T., Kaneko K., (2008), Development of porosity in carbons from yeast grains by activation with alkali metal carbonates, *J Colloid Interface Sci.* 319, 381–383

Wang XH, Chen HP, Ding XJ, Yang HP, Zhang SH, Shen YQ, (2009), Properties of gas and char from microwave pyrolysis of pine sawdust, *BioResources* 4, 946-959.

Yeletsky P.M., Yakovlev V.A., Mel'gunov M.S., Parmon V.N., (2009), Synthesis of mesoporous carbons by leaching out natural silica templates of rice husk, *Microporous and Mesoporous Materials* 121, 34–40

Zhang F., Wang K.X., Li G.D., Chen J.S., (2009), Hierarchical porous carbon derived from rice straw for lithium ion batteries with high-rate performance, *Electrochem. Commun.*, 11, 130-133.

Zhang TY., Walawendera, WP, Fana L.T., Fan MH, Daugaard D., Brown R.C., (2004), Preparation of activated carbon from forest and agricultural residues through CO₂ activation, *Chem. Eng. J.* 105, 53–59,

Zhu YW, Murali S., Stoller M.D., Ganesh K. J., Cai WW, Ruoff RS, (2011), Carbon-Based Supercapacitors Produced by Activation of Graphene *Science* 332, 1537-1539



Dr. Zhengrong Gu is an Assistant Professor in the Department of Agricultural and Biosystems Engineering at South Dakota State University (SDSU). Currently, Dr. Gu is a PI of the USDA (NIFA) project that focusing on innovative carbon materials from thermochemically generated biochar. Dr. Gu has more than 15 year experience in carbon materials preparation and application. Dr. Gu has published one textbook of “Activated Carbon” in 2008.



Ms. Xiaomin Wang is a Research Associate in Agricultural and Biosystems Engineering Dept. at SDSU. She is working on carbon materials preparation with chemical activation, microwave and hydrothermal pathways as well as ultrasonic treatment in the project funded by USDA.

Peer Review: This article has been internationally peer-reviewed and accepted for publication according to the guidelines given at the journal's website.